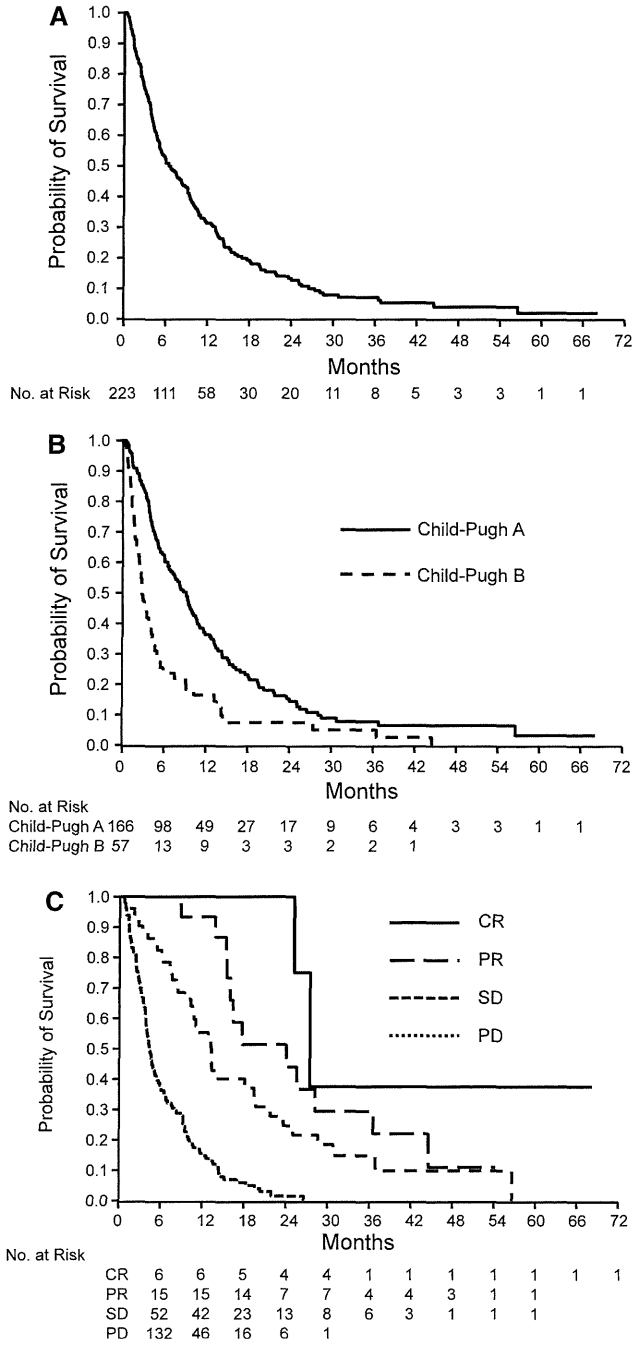

Fig. 2 Kaplan–Meier analysis of overall survival (**a**); stratified based on Child–Pugh classification (**b**) and response to treatment (**c**). *CR* complete response, *PR* partial response, *SD* stable disease, *PD* progressive disease

with CR, PR, SD, and PD were 27.4, 24.0, 13.2, and 4.4 months, respectively (Fig. 2c, $P < 0.001$). Based on a univariate analysis, the following factors were significantly associated with shorter survival time: ECOG performance status >0, Child–Pugh class B, and presence of macroscopic vascular invasion (Table 3). A multivariate analysis showed that all of these factors were also independent prognostic factors (Table 4).

Table 3 Predictors of overall survival: univariate analysis ($n = 223$)

Variable	Hazard ratio (95 % CI)	*P*
Age (years) >65	1.01 (0.76–1.35)	0.94
Male sex	1.03 (0.73–1.45)	0.87
ECOG performance status >0	1.73 (1.25–2.39)	<0.001
HBsAg, positive	0.87 (0.63–1.20)	0.38
Anti HCVAb, positive	1.06 (0.80–1.42)	0.68
Child–Pugh class B versus A	2.12 (1.54–2.92)	<0.001
Platelet count >127,000/μL	1.25 (0.94–1.67)	0.13
BCLC stage C	1.46 (0.89–2.41)	0.14
Viable intrahepatic lesion, present	1.85 (0.76–4.49)	0.17
Macroscopic vascular invasion, present	1.37 (1.03–1.83)	0.03
Extrahepatic metastasis, present	1.35 (0.97–1.87)	0.08
Previous chemotherapy, present	1.16 (0.86–1.55)	0.34

Table 4 Predictors of overall survival: multivariate analysis ($n = 223$)

Variable	Hazard ratio (95 % CI)	*P*
ECOG performance status >0	1.46 (1.04–2.05)	0.03
Child–Pugh class B	1.83 (1.31–2.55)	<0.001
Macroscopic vascular invasion, present	1.39 (1.03–1.88)	0.03
Extrahepatic metastasis, present	1.35 (0.96–1.92)	0.09

Table 5 Safety profile

	Grade 1–2, *n* (%)	Grade 3–4, *n* (%)
Leukopenia	25 (11.2)	31 (13.9)
Anemia	0 (0)	1 (0.4)
Thrombocytopenia	20 (9.0)	13 (5.8)
Stomatitis	11 (4.9)	3 (1.3)
Anorexia	2 (0.9)	1 (0.4)
Diarrhea	2 (0.9)	0 (0)
Skin rash	2 (0.9)	1 (0.4)

Safety

Adverse events graded as 3 or 4 were observed in 28 (12.6 %) patients. The incidence of major adverse events is presented in Table 5. The major grade 3–4 adverse events were leucopenia (13.9 %) and thrombocytopenia (5.8 %). A common non-hematological toxicity was stomatitis (6.2 %, any grade). Fever, which was mostly low-grade, occurred in about 90 % of the patients, usually after the first administration of peginterferon, and was gradually

attenuated during subsequent administrations. Elevations in bilirubin, AST, and ALT levels from baseline occurred in 7.6 % of patients, although most cases of such elevation occurred due to progression of the intrahepatic lesion, and not due to the treatment itself. There were no catheter-related problems, including infection or occlusion. No treatment-related deaths occurred.

Discussion

Wadler et al. first reported combination therapy with intravenous 5-FU and subcutaneous interferon for a malignant neoplasm. They treated 30 patients with advanced colorectal cancer using this protocol [19]. However, the following phase III trial failed to establish the efficacy of the treatment [20]. Subsequently, Patt et al. [21] reported systemic combination therapy for HCC patients, reporting that the treatment induced a decrease of more than 50 % in the size of each measurable lesion in 18 % of the treated patients. Since then, several studies have demonstrated the efficacy of combination therapy of intraarterial 5-FU and subcutaneous interferon for patients with advanced HCC with portal venous invasion, reporting response rates of 44–63 % [13, 22, 23]. Furthermore, other studies have revealed the mechanism underlying the antitumor effects of this combination therapy [24–31]. However, only a case series of a small number of patients has reported on this systemic combination therapy in HCC patients [32]. The present study is the first report of this therapy in a large number of patients ($n = 223$).

In the past, systemic chemotherapy for advanced HCC using various cytotoxic agents, such as doxorubicin, 5-FU, cisplatin, and etoposide, has been investigated. However, few agents showed response rates above 20 %, and the number of patients included in those studies was small. Furthermore, no regimens demonstrated convincing survival benefits in phase III trials [33, 34]. Single-agent 5-FU [35–37] and related drugs such as eniluracil/5-FU [38, 39] and uracil/tegafur [40, 41] showed low response rates. An impressive result came from phase II and phase III studies of PIAF (combination of cisplatin, interferon alfa, doxorubicin, and 5-FU). The response rates of these studies were 26 and 20.9 %, respectively [42, 43], which were actually better than that of the present study, although the number of patients was small and the characteristics of the patients differed from those in our study.

At present, sorafenib is the standard treatment for advanced HCC with extrahepatic metastasis or vascular invasion. Before the availability of sorafenib, we treated such patients with a combination of systemic intravenous 5-FU and subcutaneous interferon. The MSTs in the SHARP study and the Asian-Pacific study of sorafenib (both randomized controlled trials) were 10.7 and 6.5 months, respectively, whereas the MST in the present study was 6.5 months. However, both these trials of sorafenib consisted only of Child–Pugh class A patients, and the MSTs in these two studies were comparable to the MST of the Child–Pugh class A patients in our study (9.2 months). The disease-control rate in our study was 32.7 %, which was comparable to that of sorafenib (43 % in the SHARP study; 35.3 % in the Asian-Pacific study). Moreover, there were no complete responders in either of these randomized controlled trials, and the response rates were also low (2 % in the SHARP study; 3.3 % in the Asian-Pacific study). On the other hand, in the present study, six (2.7 %) patients achieved a complete response, and the response rate of 9.4 % was higher than that in these two studies. Thus, the combination of intravenous 5-FU and subcutaneous interferon is worth consideration as a choice of treatment for advanced HCC.

The response rate of 52.6 % that we observed in our previous study where we treated HCC patients with portal venous invasion with a combination of intraarterial 5-FU and subcutaneous interferon [13] was much better than that observed here. This may be partly because the local concentration of 5-FU in the liver is higher after intraarterial infusion than after systemic administration. However, systemic rather than intraarterial administration is appropriate for patients with extrahepatic metastases because intraarterially administered 5-FU is substantially removed by the liver in the first pass [44, 45].

In our previous study [13], we combined interferon alfa, not pegylated, with the intraarterial administration of 5-FU. Here, we combined pegylated interferon alfa with the systemic administration of 5-FU mainly because of the convenience in an outpatient setting. Whereas non-pegylated interferon needs to be administered three times a week, pegylated interferon requires only once-a-week administration.

Cirrhotic patients have lower clearance rates of 5-FU than non-cirrhotic patients [46]. Thus, such patients with poor liver function may have more severe adverse events. However, there were few serious adverse events in the present study, although as many as 25.6 % of the patients were Child–Pugh class B. Although grade 3 or 4 leucopenia and thrombocytopenia were observed, the baseline white blood cell and platelet counts in the patients with these events were almost always low because of background cirrhosis, and they were able to continue to receive treatment. In addition, we did not observe any serious adverse events in relation to infection.

According to our data, ECOG performance status, Child–Pugh classification, and the presence of vascular invasion were independent prognostic factors. This is consistent with our previous study findings on the prognosis of patients with

extrahepatic metastasis of HCC [47]. In the present study, we also analyzed prognosis as stratified by treatment response, and better treatment response resulted in better prognosis. This point is to be confirmed in future prospective studies.

The combination therapy described in the present study was performed before the advent of sorafenib. It will now be important to evaluate the efficacy of this combination therapy in cases of sorafenib failure. It is also necessary to assess the efficacy and safety of this treatment, as well as that of sorafenib, for patients with poor liver function [48, 49].

In conclusion, the combination of continuous intravenous infusion of 5-FU and subcutaneous peginterferon alfa-2a was well tolerated and showed promising efficacy in a subset of patients with advanced HCC. Further studies; for example validating the efficacy of this treatment in patients with sorafenib failure and conducting a randomized controlled trial comparing this treatment with sorafenib, are needed to definitively establish the usefulness of this treatment.

Acknowledgments This work was supported in part by Health Sciences Research Grants of The Ministry of Health, Labour and Welfare of Japan (Research on Hepatitis).

Conflict of interest Kazuhiko Koike received lecture fees and grant support from Chugai Pharmaceutical Co., Ltd.

References

1. Parkin DM, Bray F, Ferlay J, Pisani P. Global cancer statistics, 2002. CA Cancer J Clin. 2005;55(2):74–108.
2. Matsuda T, Marugame T, Kamo K, Katanoda K, Ajiki W, Sobue T. Cancer incidence and incidence rates in Japan in 2003: based on data from 13 population-based cancer registries in the Monitoring of Cancer Incidence in Japan (MCIJ) Project. Jpn J Clin Oncol. 2009;39(12):850–8.
3. Shiratori Y, Shiina S, Imamura M, Kato N, Kanai F, Okudaira T, et al. Characteristic difference of hepatocellular carcinoma between hepatitis B- and C-viral infection in Japan. Hepatology. 1995;22(4 Pt 1):1027–33.
4. Okuda K, Ohtsuki T, Obata H, Tomimatsu M, Okazaki N, Hasegawa H, et al. Natural history of hepatocellular carcinoma and prognosis in relation to treatment. Study of 850 patients. Cancer. 1985;56(4):918–28.
5. Arii S, Yamaoka Y, Futagawa S, Inoue K, Kobayashi K, Kojiro M, et al. Results of surgical and nonsurgical treatment for small-sized hepatocellular carcinomas: a retrospective and nationwide survey in Japan. The Liver Cancer Study Group of Japan. Hepatology. 2000;32(6):1224–9.
6. Shiina S, Tagawa K, Niwa Y, Unuma T, Komatsu Y, Yoshiura K, et al. Percutaneous ethanol injection therapy for hepatocellular carcinoma: results in 146 patients. AJR Am J Roentgenol. 1993; 160(5):1023–8.
7. Llovet JM, Real MI, Montana X, Planas R, Coll S, Aponte J, et al. Arterial embolisation or chemoembolisation versus symptomatic treatment in patients with unresectable hepatocellular carcinoma: a randomised controlled trial. Lancet. 2002;359(9319):1734–9.
8. Shiina S, Teratani T, Obi S, Sato S, Tateishi R, Fujishima T, et al. A randomized controlled trial of radiofrequency ablation with ethanol injection for small hepatocellular carcinoma. Gastroenterology. 2005;129(1):122–30.
9. Mazzaferro V, Regalia E, Doci R, Andreola S, Pulvirenti A, Bozzetti F, et al. Liver transplantation for the treatment of small hepatocellular carcinomas in patients with cirrhosis. N Engl J Med. 1996;334(11):693–9.
10. Shiina S, Tateishi R, Arano T, Uchino K, Enooku K, Nakagawa H, et al. Radiofrequency ablation for hepatocellular carcinoma: 10-year outcome and prognostic factors. Am J Gastroenterol 2011 [Epub ahead of print].
11. Llovet JM, Ricci S, Mazzaferro V, Hilgard P, Gane E, Blanc JF, et al. Sorafenib in advanced hepatocellular carcinoma. N Engl J Med. 2008;359(4):378–90.
12. Cheng AL, Kang YK, Chen Z, Tsao CJ, Qin S, Kim JS, et al. Efficacy and safety of sorafenib in patients in the Asia-Pacific region with advanced hepatocellular carcinoma: a phase III randomised, double-blind, placebo-controlled trial. Lancet Oncol. 2009;10(1):25–34.
13. Obi S, Yoshida H, Toune R, Unuma T, Kanda M, Sato S, et al. Combination therapy of intraarterial 5-fluorouracil and systemic interferon-alpha for advanced hepatocellular carcinoma with portal venous invasion. Cancer. 2006;106(9):1990–7.
14. Oken MM, Creech RH, Tormey DC, Horton J, Davis TE, McFadden ET, et al. Toxicity and response criteria of the Eastern Cooperative Oncology Group. Am J Clin Oncol. 1982;5(6):649–55.
15. Therasse P, Arbuck SG, Eisenhauer EA, Wanders J, Kaplan RS, Rubinstein L, et al. New guidelines to evaluate the response to treatment in solid tumors. European Organization for Research and Treatment of Cancer, National Cancer Institute of the United States, National Cancer Institute of Canada. J Natl Cancer Inst. 2000;92(3):205–16.
16. Torzilli G, Minagawa M, Takayama T, Inoue K, Hui AM, Kubota K, et al. Accurate preoperative evaluation of liver mass lesions without fine-needle biopsy. Hepatology. 1999;30(4):889–93.
17. Bruix J, Sherman M. Management of hepatocellular carcinoma. Hepatology. 2005;42(5):1208–36.
18. Llovet JM, Burroughs A, Bruix J. Hepatocellular carcinoma. Lancet. 2003;362(9399):1907–17.
19. Wadler S, Schwartz EL, Goldman M, Lyver A, Rader M, Zimmerman M, et al. Fluorouracil and recombinant alfa-2a-interferon: an active regimen against advanced colorectal carcinoma. J Clin Oncol. 1989;7(12):1769–75.
20. Greco FA, Figlin R, York M, Einhorn L, Schilsky R, Marshall EM, et al. Phase III randomized study to compare interferon alfa-2a in combination with fluorouracil versus fluorouracil alone in patients with advanced colorectal cancer. J Clin Oncol. 1996; 14(10):2674–81.
21. Patt YZ, Yoffe B, Charnsangavej C, Pazdur R, Fischer H, Cleary K, et al. Low serum alpha-fetoprotein level in patients with hepatocellular carcinoma as a predictor of response to 5-FU and interferon-alpha-2b. Cancer. 1993;72(9):2574–82.
22. Sakon M, Nagano H, Dono K, Nakamori S, Umeshita K, Yamada A, et al. Combined intraarterial 5-fluorouracil and subcutaneous interferon-alpha therapy for advanced hepatocellular carcinoma with tumor thrombi in the major portal branches. Cancer. 2002;94(2):435–42.
23. Ota H, Nagano H, Sakon M, Eguchi H, Kondo M, Yamamoto T, et al. Treatment of hepatocellular carcinoma with major portal vein thrombosis by combined therapy with subcutaneous interferon-alpha and intra-arterial 5-fluorouracil; role of type 1 interferon receptor expression. Br J Cancer. 2005;93(5):557–64.
24. Damdinsuren B, Nagano H, Sakon M, Kondo M, Yamamoto T, Umeshita K, et al. Interferon-beta is more potent than interferon-alpha in inhibition of human hepatocellular carcinoma cell

growth when used alone and in combination with anticancer drugs. Ann Surg Oncol. 2003;10(10):1184–90.
25. Eguchi H, Nagano H, Yamamoto H, Miyamoto A, Kondo M, Dono K, et al. Augmentation of antitumor activity of 5-fluorouracil by interferon alpha is associated with up-regulation of p27Kip1 in human hepatocellular carcinoma cells. Clin Cancer Res. 2000;6(7):2881–90.
26. Moriyama M, Hoshida Y, Kato N, Otsuka M, Yoshida H, Kawabe T, et al. Genes associated with human hepatocellular carcinoma cell chemosensitivity to 5-fluorouracil plus interferon-alpha combination chemotherapy. Int J Oncol. 2004;25(5):1279–87.
27. Kondo M, Nagano H, Wada H, Damdinsuren B, Yamamoto H, Hiraoka N, et al. Combination of IFN-alpha and 5-fluorouracil induces apoptosis through IFN-alpha/beta receptor in human hepatocellular carcinoma cells. Clin Cancer Res. 2005;11(3): 1277–86.
28. Takaoka A, Hayakawa S, Yanai H, Stoiber D, Negishi H, Kikuchi H, et al. Integration of interferon-alpha/beta signalling to p53 responses in tumour suppression and antiviral defence. Nature. 2003;424(6948):516–23.
29. Nagano H, Miyamoto A, Wada H, Ota H, Marubashi S, Takeda Y, et al. Interferon-alpha and 5-fluorouracil combination therapy after palliative hepatic resection in patients with advanced hepatocellular carcinoma, portal venous tumor thrombus in the major trunk, and multiple nodules. Cancer. 2007;110(11):2493–501.
30. Yamamoto T, Nagano H, Sakon M, Wada H, Eguchi H, Kondo M, et al. Partial contribution of tumor necrosis factor-related apoptosis-inducing ligand (TRAIL)/TRAIL receptor pathway to antitumor effects of interferon-alpha/5-fluorouracil against hepatocellular carcinoma. Clin Cancer Res. 2004;10(23):7884–95.
31. Nakamura M, Nagano H, Sakon M, Yamamoto T, Ota H, Wada H, et al. Role of the Fas/FasL pathway in combination therapy with interferon-alpha and fluorouracil against hepatocellular carcinoma in vitro. J Hepatol. 2007;46(1):77–88.
32. Patt YZ, Hassan MM, Lozano RD, Brown TD, Vauthey JN, Curley SA, et al. Phase II trial of systemic continuous fluorouracil and subcutaneous recombinant interferon alfa-2b for treatment of hepatocellular carcinoma. J Clin Oncol. 2003;21(3):421–7.
33. Burroughs A, Hochhauser D, Meyer T. Systemic treatment and liver transplantation for hepatocellular carcinoma: two ends of the therapeutic spectrum. Lancet Oncol. 2004;5(7):409–18.
34. Nowak AK, Chow PK, Findlay M. Systemic therapy for advanced hepatocellular carcinoma: a review. Eur J Cancer. 2004;40(10): 1474–84.
35. Link JS, Bateman JR, Paroly WS, Durkin WJ, Peters RL. 5-Flourouracil in hepatocellular carcinoma: report of twenty-one cases. Cancer. 1977;39(5):1936–9.
36. Zaniboni A, Simoncini E, Marpicati P, Marini G. Phase II study of 5-fluorouracil (5-FU) and high dose folinic acid (HDFA) in hepatocellular carcinoma. Br J Cancer. 1988;57(3):319.
37. Tetef M, Doroshow J, Akman S, Coluzzi P, Leong L, Margolin K, et al. 5-Fluorouracil and high-dose calcium leucovorin for hepatocellular carcinoma: a phase II trial. Cancer Invest. 1995; 13(5):460–3.
38. Llovet JM, Ruff P, Tassopoulos N, Castells L, Bruix J, El-Hariry I, et al. A phase II trial of oral eniluracil/5-fluorouracil in patients with inoperable hepatocellular carcinoma. Eur J Cancer. 2001; 37(11):1352–8.
39. Benson AB 3rd, Mitchell E, Abramson N, Klencke B, Ritch P, Burnhan JP, et al. Oral eniluracil/5-fluorouracil in patients with inoperable hepatocellular carcinoma. Ann Oncol. 2002;13(4): 576–81.
40. Mani S, Schiano T, Garcia JC, Ansari RH, Samuels B, Sciortino DF, et al. Phase II trial of uracil/tegafur (UFT) plus leucovorin in patients with advanced hepatocellular carcinoma. Invest New Drugs. 1998;16(3):279–83.
41. Ishikawa T, Ichida T, Sugitani S, Tsuboi Y, Genda T, Sugahara S, et al. Improved survival with oral administration of enteric-coated tegafur/uracil for advanced stage IV-A hepatocellular carcinoma. J Gastroenterol Hepatol. 2001;16(4):452–9.
42. Leung TW, Patt YZ, Lau WY, Ho SK, Yu SC, Chan AT, et al. Complete pathological remission is possible with systemic combination chemotherapy for inoperable hepatocellular carcinoma. Clin Cancer Res. 1999;5(7):1676–81.
43. Yeo W, Mok TS, Zee B, Leung TW, Lai PB, Lau WY, et al. A randomized phase III study of doxorubicin versus cisplatin/interferon alpha-2b/doxorubicin/fluorouracil (PIAF) combination chemotherapy for unresectable hepatocellular carcinoma. J Natl Cancer Inst. 2005;97(20):1532–8.
44. Ensminger WD, Rosowsky A, Raso V, Levin DC, Glode M, Come S, et al. A clinical-pharmacological evaluation of hepatic arterial infusions of 5-fluoro-2′-deoxyuridine and 5-fluorouracil. Cancer Res. 1978;38(11 Pt 1):3784–92.
45. Goldberg JA, Kerr DJ, Watson DG, Willmott N, Bates CD, McKillop JH, et al. The pharmacokinetics of 5-fluorouracil administered by arterial infusion in advanced colorectal hepatic metastases. Br J Cancer. 1990;61(6):913–5.
46. Ueno H, Okada S, Okusaka T, Ikeda M, Kuriyama H. Phase I and pharmacokinetic study of 5-fluorouracil administered by 5-day continuous infusion in patients with hepatocellular carcinoma. Cancer Chemother Pharmacol. 2002;49(2):155–60.
47. Uchino K, Tateishi R, Shiina S, Kanda M, Masuzaki R, Kondo Y, et al. Hepatocellular carcinoma with extrahepatic metastasis: clinical features and prognostic factors. Cancer. 2011;117(19): 4475–83.
48. Worns MA, Weinmann A, Pfingst K, Schulte-Sasse C, Messow CM, Schulze-Bergkamen H, et al. Safety and efficacy of sorafenib in patients with advanced hepatocellular carcinoma in consideration of concomitant stage of liver cirrhosis. J Clin Gastroenterol. 2009;43(5):489–95.
49. Pinter M, Sieghart W, Graziadei I, Vogel W, Maieron A, Konigsberg R, et al. Sorafenib in unresectable hepatocellular carcinoma from mild to advanced stage liver cirrhosis. Oncologist. 2009;14(1):70–6.

Hepatology Research

Hepatology Research 2012 doi: 10.1111/j.1872-034X.2012.01044.x

Original Article

Clinical utility of serum fucosylated hemopexin in Japanese patients with hepatocellular carcinoma

Sayo Kobayashi,[1] Kazuhiro Nouso,[1,2] Hideaki Kinugasa,[1] Yasuto Takeuchi,[1] Takeshi Tomoda,[1] Koji Miyahara,[1] Hiroaki Hagihara,[1] Kenji Kuwaki,[1] Hideki Onishi,[1,2] Shinichiro Nakamura,[1] Fusao Ikeda,[1,2] Yasuhiro Miyake,[1] Hidenori Shiraha,[1] Akinobu Takaki[1] and Kazuhide Yamamoto[1]

Departments of [1]Gastroenterology and Hepatology, and [2]Molecular Hepatology, Okayama University Graduate School of Medicine, Dentistry and Pharmaceutical Sciences, Okayama, Japan

Aim: Hepatocellular carcinoma (HCC) is a common clinical problem all over the world. Fucosylated hemopexin (Fuc-Hpx) is a newly reported glycoprotein for the diagnosis of HCC, however, its clinical implications are unclear. The aim of this study was to elucidate the clinical utility of Fuc-Hpx in Japanese patients with HCC.

Methods: The sera from 331 HCC patients, 45 with liver cirrhosis (LC), 85 with chronic hepatitis (CH) and 22 healthy people were examined for the expression of Fuc-Hpx; the level was compared with clinical parameters as well as hemopexin (Hpx) expression. The expressions of Fuc-Hpx in 12 HCC tissues and corresponding adjacent non-cancerous liver tissues were also examined.

Results: No correlation was observed between Hpx and Fuc-Hpx level. The median Fuc-Hpx levels in healthy people and CH, LC and HCC patients were 3.8, 3.7, 6.1 and 7.6 AU/mL, respectively (CH vs LC, $P = 0.002$; CH vs HCC, $P < 0.001$; LC vs HCC, $P = 0.02$). Multivariate analysis revealed that low albumin, low prothrombin time and the presence of HCC were significantly correlated with high Fuc-Hpx ($P = 0.013$, $=0.001$ and <0.001, respectively). Among the HCC patients, albumin was correlated with high Fuc-Hpx; however, none of the tumor factors, such as tumor size, tumor number and tumor stage, was correlated with Fuc-Hpx level. The expression of Fuc-Hpx in cancer tissue was not different from that in non-cancerous tissue.

Conclusion: Fuc-Hpx is a valuable biomarker for HCC but it might be a marker for hypercarcinogenic liver rather than a marker for tumor-bearing liver.

Key words: biomarker, fucosylated hemopexin, glycosylation, hepatocellular carcinoma, hypercarcinogenicity

INTRODUCTION

HEPATOCELLULAR CARCINOMA (HCC) is the fifth most common cancer and its very poor prognosis makes it the third leading cause of cancer death worldwide.[1,2] HCC accounts for over 90% of common primary liver cancer in Japan. More than 80% of HCC cases develop in patients suffering from long-lasting viral hepatitis. Recently, rising rates of diabetes, obesity and non-alcoholic steatohepatitis (NASH) have become increasingly important risk factors of future HCC incidence trends globally, particularly in developed countries.[3,4] Although HCC without hepatitis virus infection, which is difficult to survey, is increasing and the percentage of cases with viral hepatitis is decreasing in Japan, the majority of HCC patients (>80%) still suffer from either hepatitis C or hepatitis B virus (HBV) infection.[5] Many of these patients were under surveillance programs for the diagnosis of HCC, resulting in smaller tumor size at diagnosis.

While modalities of imaging diagnoses have been improving and therapeutic options have progressed, a major problem in HCC surveillance is the lack of reliable biomarkers.[4] α-Fetoprotein (AFP) is the best available biomarker with high sensitivity for HCC surveillance, but the low specificity of AFP led the

Correspondence: Dr Sayo Kobayashi, Department of Gastroenterology and Hepatology, Okayama University Graduate School of Medicine, Dentistry and Pharmaceutical Sciences, 2-5-1 Shikata-cho, Kita-ku, Okayama City, Okayama 700-8558, Japan. Email: sayo44@hotmail.co.jp

Received 20 February 2012; revision 25 March 2012; accepted 23 April 2012.

American Association for the Study of Liver Diseases Practice Guideline Committee to recommend that surveillance has to be based on ultrasound (US) examination.[6] Des-γ-carboxy prothrombin (DCP) is used widely as a HCC biomarker in Japan, but it is not popular in other countries including the USA. DCP is more closely related to tumor size with high sensitivity in the diagnosis of large HCC than AFP, but the sensitivity is low for the diagnosis of small HCC.[7] It is known that the fucosylation of glycoprotein often emerges during carcinogenesis.[8–15] The fucosylated AFP (AFP-L3) was highly specific and correlated with biological malignancy and prognosis of HCC patients.[16–19] Recent glycan analysis demonstrated the increasing fucosylation of serum glycoproteins, not only AFP but also haptoglobin, fetuin A, hemopexin (Hpx), kininogen, α-1 antitrypsin and Golgi protein 73 (GP73) with the development of HCC.[8,15]

Hemopexin is a 60-kDa glycoprotein that is one of the acute-phase reactant proteins. Besides its classical functions, such as binding and transportation of free heme in peripheral blood, a wide range of other properties of the hemopexin molecule have been described, such as antioxidant activity.[20] Hpx is produced in the liver and secreted in serum. A report from the USA demonstrated that the fucosylated form of hemopexin (Fuc-Hpx) was a good serum marker for HCC and its capacity for the diagnosis of HCC was superior to that of AFP.[8,9,21] However, the profile of glycosylation is known to be different by age, race or country of residence.[22] In addition, HCC surveillance has become popular, so the size of HCC at diagnosis is smaller in Japan than in other countries.[23,24] Thus, the aim of this study is to evaluate the clinical utilities of Fuc-Hpx in Japanese HCC patients.

METHODS

Human subjects

HUMAN SERUM SAMPLES were obtained from patients with newly developed HCC ($n = 331$), chronic hepatitis (CH, $n = 85$) or liver cirrhosis (LC, $n = 45$), who were admitted to Okayama University Hospital between 2002 and 2009, as well as from healthy volunteers ($n = 22$). The serum was collected at the time of admission, meaning that no intervention had been performed. The characteristics of the patients are summarized in Table 1. Healthy subjects did not have a past history of liver disease, cancer, or metabolic or hormonal disorder that required medication. Age is shown as median and interquartile range. The median age of HCC patients was older than that of others ($P < 0.001$). For etiology, patients with hepatitis B virus surface antigen positivity were classified as having HBV, and those with hepatitis C virus antibody were classified as hepatitis C virus (HCV). Alcohol-induced liver injury, NASH, autoimmune hepatitis or liver disease of unknown origin were classified as others. Over 80% of the patients suffered from viral infection in both the HCC and the non-HCC groups, and HCV infection was more prevalent in HCC patients than in non-HCC patients (73% vs 49%, $P < 0.001$). The changes of Fuc-

Table 1 Baseline characteristics

Disease	Healthy control	Non-HCC		HCC	*P*-value
		CH	LC		
No. of patients	22	85	45	331	
Age (years)	65 (60–71)	50 (41–55)	59 (48–66)	71 (64–76)	<0.001
Sex					
Male (%)	72	61	71	66	N.S.
Etiology (%)					
HBV/HCV/others		36/ 60/ 4	29/ 29/ 42	15/ 73/ 14	<0.001
Child–Pugh grade					
A/B or C (%)		94/ 6	53/47	79/ 21	<0.001
Stage					
I/II/III/IV (%)				31/35/20/14	

Statistical significance was set at $P < 0.05$.
CH, chronic hepatitis; HBV, positive for hepatitis B virus surface antigen; HCC, hepatocellular carcinoma; HCV, positive for hepatitis C virus antibody; LC, liver cirrhosis; others, alcohol-induced liver injury, non-alcoholic steatohepatitis, autoimmune hepatitis or liver disease of unknown origin.

Hpx between before and after curative treatments of HCC were examined in 21 cases. Nine cases were treated by local curative treatments (five surgical resection and four radiofrequency ablation). The others were treated by liver transplantation.

Hepatocellular carcinoma tissue samples and the corresponding adjacent liver tissue samples were obtained from 12 patients who received liver transplantation. Informed consent was obtained from all patients, and the study protocol conformed to the ethical guidelines of the World Medical Association Declaration of Helsinki and was approved by our institutional review board.

Diagnosis of HCC

In accordance with the AASLD 2005 Practice Guidelines, we confirmed the diagnosis of HCC by at least two dynamic imaging modalities. Typical findings were confirmed as hyperattenuation at the arterial phase and hypoattenuation at the portal phase in dynamic computed tomography (CT) or magnetic resonance imaging (MRI), and tumor staining on angiography. The nodules without these findings were diagnosed by histological examination via US-guided, fine-needle biopsy. Stage was based on the General Rules for the Clinical and Pathological Study of Primary Liver Cancer. The diagnosis of CH and LC was based on liver histology, or clinical and laboratory data including the findings of ultrasound, CT or MRI.

Sample preparation from human liver tissues

Human liver samples were extracted from 50 mg of frozen tissues. Briefly, samples were homogenized with 250 μL reagent mixed CelLytic-MT (Sigma-Aldrich, St Louis, MO, USA) containing protease inhibitor. The lysed samples were centrifuged for 10 min at 4°C, 12 000–20 000 *g*, to pellet the tissue debris. The supernatant was harvested in a clean tube and used for the following studies. Protein concentration in each sample was measured by the Bradford method.

Measurement of Hpx

Serum Hpx concentrations were measured by enzyme-linked immunosorbent assay (ELISA). We used the AssayMax Human Hemopexin ELISA kit (AssayPro, St Charles, MO, USA). The samples were measured in duplicate according to the manufacturer's instructions. A microplate reader (Model 680; Bio-Rad Laboratories, Tokyo, Japan) was used for reading absorbance at 450 nm.

Lectin ELISA for Fuc-Hpx

We performed lectin ELISA for quantitative analysis of Fuc-Hpx in accordance with the method reported by Metha *et al.* with some modification.[9] Briefly, the rabbit antihuman hemopexin antibody (AssayPro) was incubated with 10 mmol/L sodium periodate to remove the fucosylation of the captured antibody at 4°C for 1 h under dark conditions. An equal volume of ethylene glycol was added and the oxidized antibody was diluted to a concentration of 10 μg/mL with sodium carbonate buffer (pH 9.5). Antibody (1 μg) was added to each well of the ELISA plate and incubated overnight at 4°C. The plate was washed five times with 0.1% Tween-20/phosphate-buffered saline 7.4 (PBS-T) and then blocked overnight with 3% bovine serum albumin/phosphate-buffered saline (PBS).

For analysis, 50 μL of serum was diluted in 50 μL of PBS with 1 μL of Immunoglobulin Inhibiting Reagent (Bioreclamation, Westbury, NY, USA) and incubated at room temperature for 45 min. The samples were added to the plate and incubated at 37°C for 1 h, followed by washing with lectin incubation buffer (10 mM Tris pH 8.0, 0.15 M NaCl, 0.1% Tween-20) five times. After that, AAL lectin (Vector Laboratories, Burlingame, CA, USA) diluted 250 times by lectin incubation buffer was applied and incubated at room temperature for 1 h. After five washes with PBS-T, AP-streptavidin (Vector Laboratories) diluted 1000 times by PBS was applied and incubated at room temperature for 1 h. After washing five times, color was developed using phosphatase substrate (KPL, Baltimore, MD, USA) and the optical density (OD) at 630 nm was measured. The concentration is expressed as arbitrary unit (AU) based on the relative concentration against a standard HCC sample and normal stock serum. The control curve of lectin-ELISA is shown in Figure 1.

Statistical analysis

The JMP ver. 8.02 software (SAS Institute, Cary, NC, USA) was used for the analyses. Continuous variables are shown as median and interquartile range. The Wilcoxon rank sum test was used to compare the continuous data and the χ^2-test was used to compare categorical data. Statistical significance was set at $P < 0.05$. Univariate analysis was performed in allpatients except healthy volunteers to identify the potential factors correlated with Fuc-Hpx in liver diseases. Variables at $P < 0.05$ in the univariate analysis were further analyzed to identify independent factors correlated with Fuc-Hpx by multivariate analysis. The variables used in the analysis

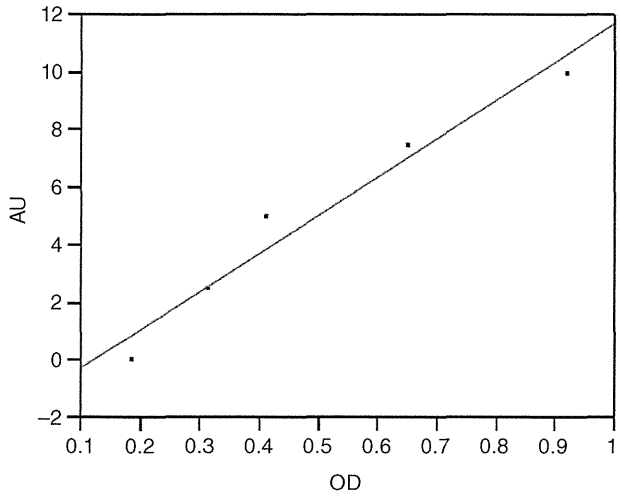

Figure 1 Control curve of lectin enzyme-linked immunoassay. The concentration is expressed as arbitrary unit (AU) based on the relative concentration against control curve. OD, optical density.

included age, sex, etiology, presence of HCC, platelet count (Plt), prothrombin time (PT), albumin (Alb), total bilirubin (T-Bil), aspartate aminotransferase (AST), alanine aminotransferase (ALT) and Child–Pugh grade. For the analysis in HCC patients, tumor markers such as AFP, AFP-L3, DCP, tumor size, tumor number, presence of portal vein tumor thrombosis (Vp) and tumor stage were added. The optimal cut-off values of most variables were set at approximate values of medians. Those of AFP, AFP-L3 and DCP were 20 ng/mL, 10% and 40 mAU/mL, respectively. Student's paired *t*-test was used for the analysis of Fuc-Hpx expression levels between HCC and adjacent liver tissues. Correlation analysis was verified at r^2 value by Pearson correlation coefficient. Diagnostic abilities in differentiating HCC from liver disease without HCC were evaluated using the areas under the receiver–operator curve (AUROC). Sensitivity, specificity and accuracy were analyzed by the McNemar test, and positive predictive value (PPV) and negative predictive value (NPV) were analyzed by Fisher's exact test. All tests were two-sided between Fuc-Hpx and another marker, and $P < 0.05$ was considered significant.

RESULTS

Relationship between serum Hpx and Fuc-Hpx

TO DETERMINE THE effect of Hpx concentration on Fuc-Hpx level, we measured both Hpx and Fuc-Hpx expressions in 18 samples simultaneously (Fig. 2). No correlation was observed between Hpx and Fuc-Hpx ($P = 0.89$). The level of Hpx was not significantly different between the non-HCC (median, 648 AU/mL; range, 488–750) and HCC groups (median, 772 AU/mL; range, 483–1022; $P = 0.16$), whereas Fuc-Hpx level was higher in the HCC group (median, 6.8 AU/mL; range, 4.9–11.0) than in the non-HCC group (median, 2.6 AU/mL; range, 0.9–4.8; $P < 0.001$). Because total Fuc-Hpx level was closely correlated with the percentage of Fuc-Hpx ($R^2 = 0.6$, $P < 0.001$) and no difference of AUROC of total and percentage of Fuc-Hpx was observed in this study population (0.84 and 0.77, respectively), we used total Fuc-Hpx level in the following analysis.

Serum Fuc-Hpx level in liver diseases

To confirm the Fuc-Hpx expression in various liver diseases, we measured it in large populations. The median value in the HCC group ($n = 331$) was 7.6 AU/mL (range, 5.6–10.8), which was significantly higher than that of the non-HCC group ($n = 130$; median, 4.6 AU/mL; range, 2.5–7.1; $P < 0.001$). A progressive increase of Fuc-Hpx was observed from that of healthy controls (median, 3.8 AU/mL; range, 0.1–5.8) through CH (median, 3.7 AU/mL; range, 1.9–6.2) to LC (median, 6.1 AU/mL; range, 4.1–8.9). Significant difference was

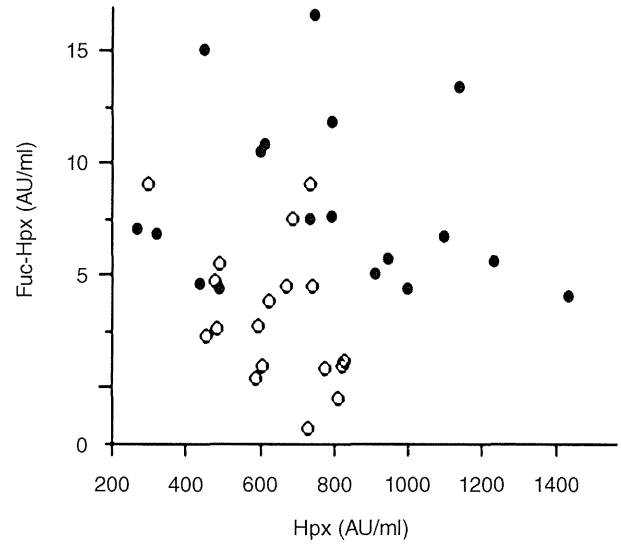

Figure 2 Relationship between serum hemopexin (Hpx) and fucosylated hemopexin (Fuc-Hpx). The data of hepatocellular carcinoma (HCC) and non-HCC are plotted by closed circles and open circles, respectively. No correlation was demonstrated between serum Hpx and Fuc-Hpx in both groups.

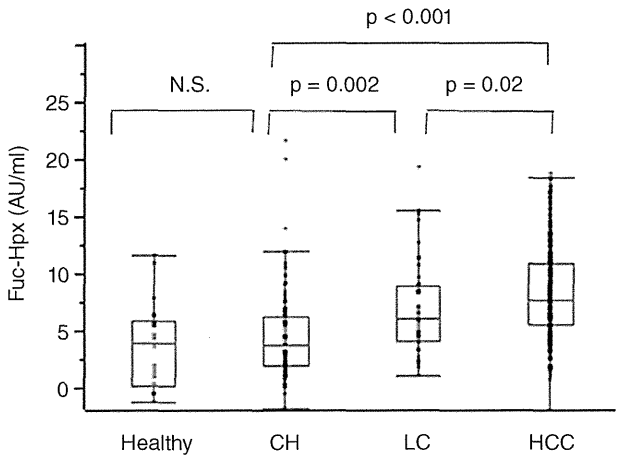

Figure 3 Serum fucosylated hemopexin (Fuc-Hpx) concentration. Serum Fuc-Hpx level increased according to the progression of the liver diseases. CH, chronic hepatitis; HCC, hepatocellular carcinoma; LC, liver cirrhosis; N.S., not significant.

observed between the HCC group and LC ($P = 0.02$) or CH group ($P < 0.001$), and between LC and CH groups ($P = 0.002$), but no difference was observed between the CH group and healthy subjects (Fig. 3). We examined Fuc-Hpx level in patients with or without HCC with the same liver function. The median was 7.7 AU/mL (range, 5.4–10.5) in the HCC group, which was significantly higher than that in the non-HCC group (median, 3.9 AU/mL; range, 2.1–6.7; $P < 0.001$) in Child–Pugh grade A patients. In Child–Pugh grade B/C patients, no difference was observed between the groups, and the median was 7.8 AU/mL (range, 6.2–11.1) and 6.6 AU/mL (range, 5.5–11.2) in the HCC group and in non-HCC group, respectively. We measured to compare Fuc-Hpx levels in 21 HCC cases before and after curative therapy. Fuc-Hpx levels in all nine cases but one who received local curative treatments did not decrease after the treatments. The median Fuc-Hpx levels before and after the treatments were 5.23 and 6.77 AU/mL, respectively. On the other hand, in nine out of 12 HCC cases who received liver transplantation, the median Fuc-Hpx level significantly decreased from 10.2 to 4.87 AU/mL ($P = 0.02$). Significant difference was observed between local curative treatment and liver transplantation ($P = 0.001$).

Factors correlated with serum Fuc-Hpx

We evaluated the relationship between serum Fuc-Hpx and clinical parameters in patients with liver diseases (Table 2). Fuc-Hpx in elderly patients and HCV-infected patients was high. High AST (≥40 IU/L) and T-Bil (≥1.0 mg/dL), and low Plt (≤10 × 10^4/μL), PT (<100%) and Alb (≤3.5 g/dL), were also correlated with high serum Fuc-Hpx level. In addition, the presence of HCC was significantly associated with high Fuc-Hpx

Table 2 Fucosylated hemopexin expression in patients with liver diseases

Variables	Fuc-Hpx, medium (range) (AU/mL)	Univariate *P*-value	Multivariate *P*-value
Age (years)			
≤65	6.2 (3.5–9.0)	<0.001	0.600
>65	7.5 (5.3–10.8)		
Sex			
Male	7.2 (4.5–10.2)	0.690	
Female	6.8 (4.5–9.7)		
Etiology			
HBV	6.3 (4.1–9.8)	0.025	0.410
HCV	7.4 (4.8–10.4)		
Others	6.2 (3.6–8.8)		
Diagnosis			
Non-HCC	4.6 (2.5–7.1)	<0.001	<0.001
HCC	7.6 (5.6–10.8)		
Plt (×10^4/μL)			
>10	6.6 (3.9–9.8)	0.002	0.800
≤10	8.1 (5.3–10.4)		
PT (%)			
≥100	6.3 (4.0–9.4)	<0.001	0.001
<100	7.9 (5.6–11.0)		
Albumin (g/dL)			
>3.5	5.8 (3.3–9.0)	<0.001	0.013
≤3.5	8.1 (6.3–11.1)		
T-Bil (mg/dL)			
<1	6.7 (4.0–9.8)	0.031	0.990
≥1	7.3 (5.3–10.5)		
AST (IU/L)			
<40	5.3 (2.8–8.4)	<0.001	
≥40	7.4 (5.4–10.3)		
ALT (IU/L)			
<40	6.5 (4.0–9.4)	0.100	
≥40	7.0 (4.8–10.0)		
Child–Pugh grade			
A	6.7 (4.2–9.8)	0.004	
B + C	7.7 (5.8–11.1)		

Statistical significance was set at $P < 0.05$.
ALT, alanine aminotransferase; AST, aspartate aminotransferase; CH, chronic hepatitis; Fuc-Hpx, fucosylated hemopexin; HBV, positive for hepatitis B virus surface antigen; HCC, hepatocellular carcinoma; HCC, hepatocellular carcinoma; HCV, positive for hepatitis C virus antibody; LC, liver cirrhosis; others, alcohol-induced liver injury, non-alcoholic steatohepatitis, autoimmune hepatitis or liver disease of unknown origin; Plt, platelet count; PT, prothrombin time; T-Bil, total bilirubin.

Table 3 Relationship between clinical parameters and fucosylated hemopexin in HCC patients

Variables	Fuc-Hpx, median (range) (AU/mL)	Univariate *P*-value	Multivariate *P*-value
Albumin (g/dL)			
>3.5	7.1 (4.5–10.3)	<0.001	0.027
≤3.5	8.1 (6.4–11.2)		
PT (%)			
≥100	7.2 (5.0–9.8)	0.004	0.053
<100	8.3 (6.1–11.4)		
AFP (ng/mL)			
<20	7.5 (5.0–10.5)	0.083	
≥20	7.8 (6.0–10.9)		
AFP-L3 (%)			
<10	7.6 (5.5–10.4)	0.379	
≥10	7.8 (6.1–11.2)		
DCP (mAU/mL)			
<40	7.4 (5.0–10.2)	0.021	0.063
≥40	8.1 (6.0–11.2)		
Tumor size (mm)			
<20	7.4 (5.5–10.1)	0.190	
≥20	8.0 (5.5–11.2)		
Tumor number			
Single	7.4 (5.0–10.4)	0.230	
Multiple	7.7 (6.1–10.9)		
Vp			
Yes	7.6 (5.5–10.4)	0.800	
No	7.7 (4.6–11.0)		
Stage			
I + II	7.5 (5.3–10.2)	0.420	
III + IV	7.7 (5.6–11.1)		

Statistical significance was set at $P < 0.05$.
AFP, α-fetoprotein; AFP-L3, fucosylated AFP; DCP, des-γ-carboxy prothrombin; Fuc-Hpx, fucosylated hemopexin; HCC, hepatocellular carcinoma; PT, prothrombin time; Vp, portal vein tumor thrombosis.

($P < 0.001$). On multivariate analysis, low Alb, low PT and the presence of HCC were significantly correlated with high Fuc-Hpx ($P = 0.013$, $P = 0.001$, and $P < 0.001$, respectively).

The relationship between Fuc-Hpx and tumor factors in combination with three variables that showed correlation with Fuc-Hpx on multivariate analysis was examined in HCC patients (Table 3). None of the tumor factors such as tumor size, tumor number, Vp or stage was correlated with Fuc-Hpx level. Fuc-Hpx was high in patients with high DCP (≥40 mAU/mL), while AFP and AFP-L3 were not correlated with Fuc-Hpx. On multivariate analysis, Alb was the only factor correlated with serum Fuc-Hpx level ($P = 0.027$).

Utility of Fuc-Hpx for the diagnosis of HCC

The accuracy, sensitivity and specificity of Fuc-Hpx for the diagnosis of HCC were 69%, 71% and 63% at a cut-off of 5.95 AU/mL, respectively (Table 4). The diagnostic accuracies of AFP and DCP in the same serum samples were 56% and 58%, sensitivities were 46% and 47%, and specificities were 87% and 91% at cut-offs of 20 ng/mL and 40.0 mAU/mL, respectively. The receiver-operator curve (ROC) of three individual markers is shown in Figure 4. The AUROC of Fuc-Hpx for the diagnosis of HCC was 0.739, which was inferior to that of AFP (0.791) but superior to DCP (0.723).

The levels of AFP and DCP gradually increased as the stage progressed, but no correlation was observed between Fuc-Hpx and the stage. The sensitivity of Fuc-Hpx was superior to that of the others in both stage I and stage II or more patients. The clinical utility of Fuc-Hpx was equivalent in both stage I and stage II or more patients as well as AFP. AUROC was statistical significantly superior to DCP in stage I.

Table 4 Utilities of tumor markers for the diagnosis of HCC

	Fuc-Hpx	AFP	DCP
All stages			
AUROC	0.739	0.791	0.723
Sensitivity (%)	71	46**	47**
Specificity (%)	63	87*:	91**
Accuracy (%)	69	56	58
PPV (%)	83	91	94
NPV (%)	46	36	37
Stage I			
AUROC	0.720	0.785	0.599*
Sensitivity (%)	75	45**	28**
Specificity (%)	63	87**	91**
Accuracy (%)	69	67	60
PPV (%)	63	76	76
NPV (%)	75	63	56
Stage II or more			
AUROC	0.737	0.802	0.785
Sensitivity (%)	71	46**	57*
Specificity (%)	63	87**	91**
Accuracy (%)	69	56	68
PPV (%)	83	91	93
NPV (%)	46	36	51

*Statistically significant difference between Fuc-Hpx and the other marker in the given group ($P < 0.05$).
**Statistically significant difference between Fuc-Hpx and the other marker in the given group ($P < 0.001$).
AFP, α-fetoprotein; AUROC, areas under the receiver-operator curve; DCP, des-γ-carboxy prothrombin; Fuc-Hpx, fucosylated hemopexin; HCC, hepatocellular carcinoma; NPV, negative predictive value; PPV, positive predictive value.

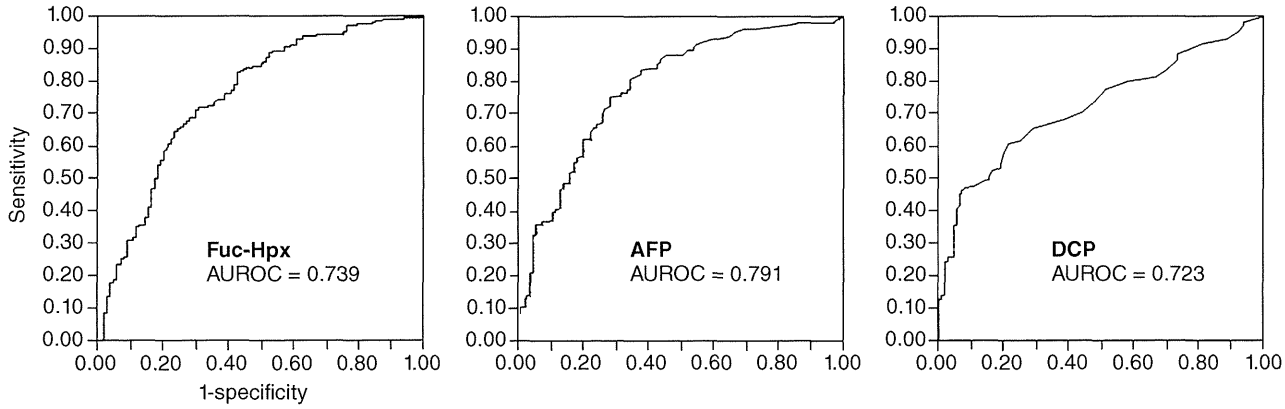

Figure 4 Receiver–operator curve of three tumor makers of hepatocellular carcinoma. The area under the receiver–operator curve (AUROC) of fucosylated hemopexin (Fuc-Hpx) for the diagnosis of hepatocellular carcinoma (HCC) was 0.739, which was inferior to that of α-fetoprotein (AFP) (0.791) but was superior to that of des-γ-carboxy prothrombin (DCP) (0.723).

The sensitivities of Fuc-Hpx + AFP and Fuc-Hpx + DCP were 84% and 74%, respectively, and the specificities were 66% and 71%, respectively. Sensitivity was improved, whereas specificity was not improved by combination with AFP or DCP.

Fuc-Hpx expression in liver tissue

The expression of Fuc-Hpx in HCC tissue was higher than that in adjacent non-cancerous liver tissue in four out of 12 HCC patients, almost equal in one patient and lower in seven patients. Median Fuc-Hpx level in HCC tissue was 6.5 AU/mL and 7.0 AU/mL in adjacent non-cancerous tissue. The difference between them was not statistically significant (Fig. 5).

DISCUSSION

SEVERAL TUMOR MARKERS of HCC have been identified, but there is no evidence indicating that the detection of HCC by these markers precedes clinical imaging diagnosis. However, the diagnostic accuracy of the radiological tools is dependent on tumor size and this approach is expensive.[25] Moreover, US examination is affected by the skill of individual operators. Therefore, it is necessary to find non-invasive, reliable markers for detecting or predicting HCC.

The expression of Fuc-Hpx increased according to the progression of liver disease from hepatitis, cirrhosis, to HCC, and albumin, PT and the presence of HCC were major factors to determine the expression level. However, we did not observe any correlations between Fuc-Hpx and tumor factors such as tumor size or tumor number. The result is quite different from those of conventional tumor markers such as AFP and DCP. From the analysis of the expression in liver tissues, Fuc-Hpx was produced not only in HCC but also in non-cancerous tissue, meaning that Fuc-Hpx might be a biomarker for hypercarcinogenic liver rather than a marker for tumor-bearing liver.

Recently, glycoproteomics and glycomics have been focused on as a post-genomic research field to find

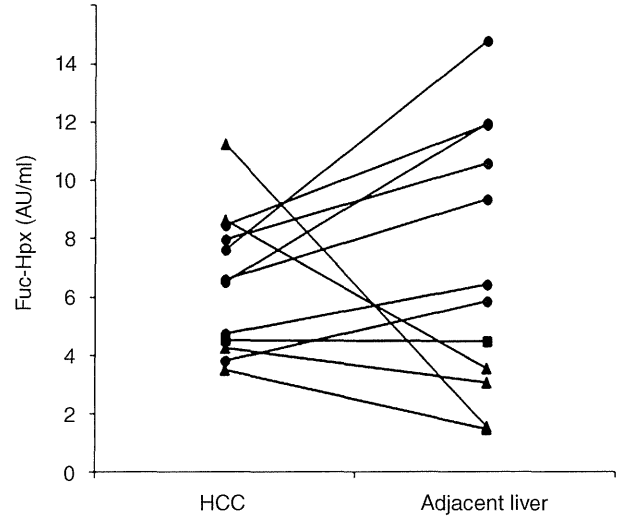

Figure 5 Fucosylated hemopexin (Fuc-Hpx) expression in liver tissue. Fuc-Hpx expressions in hepatocellular carcinoma (HCC) tissues and corresponding adjacent non-cancerous liver tissues are shown. Closed circles indicate that Fuc-Hpx was lower in cancerous tissue than in non-cancerous tissue. Closed triangles indicate that Fuc-Hpx expression was higher in cancerous tissue. Closed squares indicate that the expression was at the same level in both tissues.

diagnostic markers.[26,27] Glycosylation is involved in both physiological and pathological events, such as cell growth, migration, differentiation and tumor invasion. In particular, fucosylation of N-glycan is well known as one of the changes during carcinogenesis of various cancers.[8,14,15,28] There are several putative mechanisms of elevation of fucosylated proteins in cancers. A tumor marker of HCC, AFP-L3, was produced by core fucosylation of AFP by α-1,6-fucosyltransferase (Fut8), which is overexpressed in advanced liver diseases. However, high expression of Fut8 was also observed in non-cancerous liver cirrhotic tissues as well as HCC tissues.[29] α-1,6-Fucosylated proteins are normally rare in the blood and are enriched in the bile by proper balance of two secretion pathways of glycoproteins; one is sorting to an apical surface of hepatocytes followed by secretion into bile ducts and the other is sorting to the basolateral surface followed by secretion into blood vessels.[13] If hepatocytes become depolarized in hepatocarcinogenesis, these normal secretion pathways cannot work and, thus, fucosylated proteins are elevated in the blood.[30]

Several reports have been published dealing with the utility of Fuc-Hpx for the diagnosis of HCC.[8,9,21] They reported that Fuc-Hpx is superior to AFP, which has been a standard marker for the detection of HCC. Comunale *et al.* reported that the sensitivity and specificity of Fuc-Hpx for the diagnosis of HCC were high (both 92%) and the AUROC for Fuc-Hpx was 0.951.[9] In our study, the diagnostic ability in Japanese patients was inferior to the data described above. In a previous report, they analyzed 72 HCC patients and 280 patients without HCC; however, 248 out of 280 were non-cirrhotic patients including 20 healthy controls.[9] The AUROC decreased to 0.8665 when only cirrhotic patients were used as controls. We did not include healthy controls for AUROC analysis so the difference of the liver function in non-HCC patients might be one of the reasons for the difference of AUROC between the studies. In addition, the race was different, the median age was higher and the etiology was different; hepatitis virus infection was a major cause of liver injury in our research, while alcoholism was the main etiology in previous reports. Although it is not clear whether these differences affect the diagnostic utility, it is possible that albumin and PT, which are factors correlated with Fuc-Hpx expression, are different between the studies, which were not precisely indicated in other reports. Despite the differences, Fuc-Hpx expression in HCC patients was high in both studies, indicating that Fuc-Hpx is an effective biomarker for HCC.

Although serum Fuc-Hpx increased in HCC patients, the expression level was not correlated with any tumor factors. Furthermore, Fuc-Hpx levels did not decrease except one case by surgical resection or radiofrequency ablation. On the other hand, in nine out of 12 cases who received liver transplantation, which replaced the hypercarcinogenic liver with normal liver, Fuc-Hpx level decreased by the treatment. The result indicated that the major source of Fuc-Hpx in blood is non-cancerous liver tissue although it might be secreted from HCC by the mechanism described above. Scarce correlation with tumor factors is a disadvantage as a conventional tumor marker. Generally, the annual incidence of HCC from LC is known to be 4–8%. On the other hand, the recurrence rate of HCC is reported at an annual rate of 20%, indicating tumor-bearing liver is hypercarcinogenic. We conjectured that the difference of Fuc-Hpx between LC and HCC might correspond to the hypercarcinogenic status mentioned above. We inferred that a high level of Fuc-Hpx might not be shown in HCC but could be shown in hypercarcinogenic liver. In the present study, we could not confirm how effective Fuc-Hpx was as a hypercarcinogenic marker because it was not examined prospectively. If we assumed that the AUROC for the diagnosis of HCC was a surrogate marker of hypercarcinogenicity, the ability of Fuc-Hpx (0.73) was higher than that of Alb, Plt count and Child–Pugh grade (0.53, 0.66 and 0.67, respectively)

In this study, we demonstrated that Fuc-Hpx could be an effective biomarker of HCC. Future prospective research is necessary to verify the utility of Fuc-Hpx as a marker for hypercarcinogenic liver.

ACKNOWLEDGMENTS

WE THANK ALL staff members of the Department of Gastroenterology and Hepatology, and Department of Molecular Hepatology, Okayama University Graduate School of Medicine, Dentistry and Pharmaceutical Sciences, for providing baseline data and helpful discussions.

REFERENCES

1 Jemal A, Bray F, Center MM, Ferlay J, Ward E, Forman D. Global cancer statistics. *CA Cancer J Clin* 2011; **61** (2): 69–90.
2 Venook AP, Papandreou C, Furuse J, de Guevara LL. The incidence and epidemiology of hepatocellular carcinoma: a global and regional perspective. *Oncologist* 2010; **15** (Suppl 4): 5–13.

3 Davila JA, Morgan RO, Shaib Y, McGlynn KA, El-Serag HB. Hepatitis C infection and the increasing incidence of hepatocellular carcinoma: a population-based study. *Gastroenterology* 2004; **127** (5): 1372–80.
4 Gomaa AI, Khan SA, Leen EL, Waked I, Taylor-Robinson SD. Diagnosis of hepatocellular carcinoma. *World J Gastroenterol* 2009; **15** (11): 1301–14.
5 Nouso K, Kobayashi Y, Nakamura S *et al.* Evolution of prognostic factors in hepatocellular carcinoma in Japan. *Aliment Pharmacol Ther* 2010; **31** (3): 407–14.
6 Bruix J, Sherman M. Management of hepatocellular carcinoma. *Hepatology* 2005; **42** (5): 1208–36.
7 Nakamura S, Nouso K, Sakaguchi K *et al.* Sensitivity and specificity of des-gamma-carboxy prothrombin for diagnosis of patients with hepatocellular carcinomas varies according to tumor size. *Am J Gastroenterol* 2006; **101** (9): 2038–43.
8 Comunale MA, Lowman M, Long RE *et al.* Proteomic analysis of serum associated fucosylated glycoproteins in the development of primary hepatocellular carcinoma. *J Proteome Res* 2006; **5** (2): 308–15.
9 Comunale MA, Wang M, Hafner J *et al.* Identification and development of fucosylated glycoproteins as biomarkers of primary hepatocellular carcinoma. *J Proteome Res* 2009; **8** (2): 595–602.
10 Liu X-E, Desmyter L, Gao C-F *et al.* N-glycomic changes in hepatocellular carcinoma patients with liver cirrhosis induced by hepatitis B virus. *Hepatology* 2007; **46** (5): 1426–35.
11 Liu Y, He J, Li C *et al.* Identification and confirmation of biomarkers using an integrated platform for quantitative analysis of glycoproteins and their glycosylations. *J Proteome Res* 2010; **9** (2): 798–805.
12 Moriwaki K. Fucosylation and gastrointestinal cancer. *World. J Hepatol* 2010; **2** (4): 151–61.
13 Tsutomu N, Shunsaku T, Akihiko K *et al.* Glycomic analyses of glycoproteins in bile and serum during Rat Hepatocarcinogenesis. *J Proteome Res* 2010; **9** (10): 4888–96.
14 Nakagawa T, Uozumi N, Nakano M *et al.* Fucosylation of N-glycans regulates the secretion of hepatic glycoproteins into bile ducts. *J Biol Chem* 2006; **281** (40): 29797–806.
15 Wang M, Long RE, Comunale MA *et al.* Novel fucosylated biomarkers for the early detection of hepatocellular carcinoma. *Cancer Epidemiol Biomarkers Prev* 2009; **18** (6): 1914–21.
16 Kobayashi M, Kuroiwa T, Suda T *et al.* Fucosylated fraction of alpha-fetoprotein, L3, as a useful prognostic factor in patients with hepatocellular carcinoma with special reference to low concentrations of serum alpha-fetoprotein. *Hepatol Res* 2007; **37** (11): 914–22.
17 Miyaaki H, Nakashima O, Kurogi M, Eguchi K, Kojiro M. Lens culinaris agglutinin-reactive α-fetoprotein and protein induced by vitamin K absence II are potential indicators of a poor prognosis: a histopathological study of surgically resected hepatocellular carcinoma. *J Gastroenterol* 2007; **42** (12): 962–8.
18 Nouso K, Kobayashi Y, Nakamura S *et al.* Prognostic importance of fucosylated alpha-fetoprotein in hepatocellular carcinoma patients with low alpha-fetoprotein. *J Gastroenterol Hepatol* 2011; **26** (7): 1195–200.
19 Tada T, Kumada T, Toyoda H *et al.* Relationship between Lens culinaris agglutinin-reactive alpha-fetoprotein and pathologic features of hepatocellular carcinoma. *Liver Int* 2005; **25** (4): 848–53.
20 Delanghe JR, Langlois MR. Hemopexin: a review of biological aspects and the role in laboratory medicine. *Clin Chim Acta* 2001; **312** (1–2): 13–23.
21 Debruyne EN, Vanderschaeghe D, Van Vlierberghe H, Vanhecke A, Callewaert N, Delanghe JR. Diagnostic value of the hemopexin n-glycan profile in hepatocellular carcinoma patients. *Clin Chem* 2010; **56** (5): 823–31.
22 Ruhaak LR, Uh HW, Beekman M *et al.* Plasma protein N-glycan profiles are associated with calendar age, familial longevity and health. *J Proteome Res* 2011; **10**: 1667–74.
23 Llovet JM. Updated treatment approach to hepatocellular carcinoma. *J Gastroenterol* 2005; **40** (3): 225–35.
24 Makuuchi M, Kokudo N, Arii S *et al.* Development of evidence-based clinical guidelines for the diagnosis and treatment of hepatocellular carcinoma in Japan. *Hepatol Res* 2008; **38** (1): 37–51.
25 Colombo M. Screening and diagnosis of hepatocellular carcinoma. *Liver Int* 2009; **29** (Suppl 1): 143–7.
26 Amano M, Nishimura S. Large-scale glycomics for discovering cancer-associated N-glycans by integrating glycoblotting and mass spectrometry. *Methods Enzymol* 2010; **478**: 109–25.
27 Callewaert N, Vlierberghe HV, Hecke AV, Laroy W, Delanghe J, Contreras R. Noninvasive diagnosis of liver cirrhosis using DNA sequencer–based total serum protein glycomics. *Nat Med* 2004; **10** (4): 429–34.
28 Okuyama N, Ide Y, Nakano M *et al.* Fucosylated haptoglobin is a novel marker for pancreatic cancer: a detailed analysis of the oligosaccharide structure and a possible mechanism for fucosylation. *Int J Cancer* 2006; **118** (11): 2803–8.
29 Noda K, Miyoshi E, Uozumi N *et al.* Gene expression of alpha1-6 fucosyltransferase in human hepatoma tissues: a possible implication for increased fucosylation of alpha-fetoprotein. *Hepatology* 1998; **28** (4): 944–52.
30 Blomme B, Van Steenkiste C, Vanhuysse J, Colle I, Callewaert N, Van Vlierberghe H. Impact of elevation of total bilirubin level and etiology of the liver disease on serum N-glycosylation patterns in mice and humans. *Am J Physiol Gastrointest Liver Physiol* 2010; **298** (5): G615–24.

Hypovascular Nodules in Patients with Chronic Liver Disease: Risk Factors for Development of Hypervascular Hepatocellular Carcinoma[1]

Tomoko Hyodo, MD
Takamichi Murakami, MD, PhD
Yasuharu Imai, MD, PhD
Masahiro Okada, MD, PhD
Masatoshi Hori, MD, PhD
Yuki Kagawa, MD, PhD
Sachiyo Kogita, MD
Seishi Kumano, MD, PhD
Masatoshi Kudo, MD, PhD
Teruhito Mochizuki, MD

Purpose: To identify patient characteristics and magnetic resonance (MR) imaging findings associated with subsequent hypervascularization in hypovascular nodules that show hypointensity on hepatobiliary phase gadoxetic acid–enhanced MR images in patients with chronic liver diseases.

Materials and Methods: Institutional review board approval was obtained, and informed consent was waived. At multiple follow-up gadoxetic acid–enhanced MR imaging examinations of 68 patients, 160 hypovascular nodules were retrospectively reviewed. A Cox regression model for hypervascularization was developed to explore the association of baseline characteristics, including patient factors (Child-Pugh classification, etiology of liver disease, history of local therapy for hepatocellular carcinoma [HCC], and coexistence of hypervascular HCC) and MR imaging findings (fat content, signal intensity on T2-weighted images, and nodule size). In addition, the growth rate was calculated as the reciprocal of tumor volume doubling time to investigate its relationship with subsequent hypervascularization by using receiver operating characteristic and Kaplan-Meier analyses.

Results: The prevalence of subsequent hypervascularization was 31% (50 of 160 nodules). Independent Cox multivariable predictors of increased risk of hypervascularization were hyperintensity on T2-weighted images (hazard ratio [HR] = 8.7; 95% confidence interval [CI]: 3.6, 20.8), previous local therapy for hypervascular HCC (HR = 5.0; 95% CI: 1.8, 13.6), Child-Pugh B cirrhosis (HR = 3.6; 95% CI: 1.4, 9.5) and coexistence of hypervascular HCC (HR = 2.0; 95% CI: 1.0, 3.8). The mean growth rate was significantly higher in nodules that showed subsequent hypervascularization than in those without hypervascularization. Kaplan-Meier analysis based on the receiver operating characteristic cutoff level (1.8×10^{-3}/day [tumor volume doubling time, 542 days]) showed that nodules with a higher growth rate had a significantly higher incidence of hypervascularization ($P = 5.2 \times 10^{-8}$, log-rank test).

Conclusion: Hyperintensity on T2-weighted images is an independent and strong risk factor at baseline for subsequent hypervascularization in hypovascular nodules in patients with chronic liver disease. Tumor volume doubling time of less than 542 days was associated with a high rate of subsequent hypervascularization.

[1] From the Departments of Radiology (T.H., T. Murakami, M.O., Y.K.) and Internal Medicine (M.K.), Kinki University Faculty of Medicine, 377-2 Ohno-Higashi, Osaka-Sayama, Osaka 589-8511, Japan; Department of Gastroenterology, Ikeda Municipal Hospital, Osaka, Japan (Y.I., S. Kogita); Department of Radiology, Osaka University Graduate School of Medicine, Suita, Japan (M.H.); Department of Radiology, Osaka Medical College, Takatsuki, Japan (S. Kumano); and Department of Diagnostic and Therapeutic Radiology, Ehime University Graduate School of Medicine, Toon, Japan (T.H., T. Mochizuki). From the 2011 RSNA Annual Meeting. Received December 16, 2011; revision requested January 30, 2012; revision received July 30; accepted August 29; final version accepted September 18. Supported by an Osaka Cancer Foundation grant. **Address correspondence to** T.H. (e-mail: *neneth@m.ehim-u.ac.jp*).

Follow-up surveillance of patients with cirrhosis has been performed to detect hepatocellular carcinoma (HCC) early enough to allow curative treatment (1). The American Association for the Study of Liver Diseases practice guidelines outline a strategy for distinguishing HCCs from other hepatic lesions of smaller than 3 cm that are identified during ultrasound (US) screening of livers in patients with cirrhosis (2). The guidelines suggest that nodules greater than 1 cm in diameter be further investigated by using dynamic contrast material–enhanced computed tomography (CT) or magnetic resonance (MR) imaging. Thus, the detection of arterial hypervascularization can justify treating the nodule as if it were HCC. For hypovascular nodules, defined as lesions that appear less enhanced than the surrounding liver both on arterial and venous phase images (2), careful monitoring (eg, repeat US at 3 months and biopsy) is recommended. However, the existing treatment guidelines do not specify the patient and tumor attributes that accurately predict subsequent hypervascularization.

Advances in Knowledge

- In patients with chronic liver disease, 31% (50 of 160) of the hypovascular nodules that showed hypointensity in the hepatobiliary phase of gadoxetic acid–enhanced MR imaging became hypervascular, which is a 1-year cumulative incidence of 25%.
- Hepatic hypovascular nodules that showed hyperintensity on T2-weighted images were at the highest risk for development of hypervascular hepatocellular carcinoma (hazard ratio, 8.7; 95% CI: 3.6, 20.8; $P < .001$).
- The higher growth rate (tumor volume doubling time, < 542 days) of a hepatic hypovascular nodule was associated with its subsequent development to hypervascular hepatocellular carcinoma.

The hepatobiliary phase of gadoxetic acid–enhanced MR imaging can allow clear visualization of hepatic focal lesions (3–6). Along with the widespread use of advanced imaging techniques, including three-dimensional T1-weighted gradient-echo sequences with high spatial resolution (7), hypovascular small nodules that show hypointensity on gadoxetic acid–enhanced hepatobiliary phase MR images are increasingly detected during HCC screening of patients with cirrhosis. Such nodules may include hypovascular well-differentiated HCCs, dysplastic nodules, and other benign nodules (8), which are difficult to distinguish, even at needle biopsy. Of these, hypovascular HCC and dysplastic nodules grow and acquire a more extensive arterial supply, and show overt stromal invasion (invasive growth of tumor tissue in portal tracts and fibrous septa), during stepwise carcinogenesis of HCC (9,10).

Previously, image-based studies suggested that hypovascular nodules containing fat or those that were greater than 10–15 mm in diameter were at high risk for development of hypervascularization (11–13). Authors of a histopathologic study (14) reported that most borderline nodules (dysplastic nodules or well-differentiated HCCs) greater than 15 mm in diameter were early HCC. Because these results were taken from findings at a single time point, further research examining the time course of the development of this change is required for the development of a better approach to follow-up of these hypovascular nodules.

Implications for Patient Care

- MR imaging findings may provide useful diagnostic information for the development of a treatment strategy for patients with hepatic hypovascular nodules.
- The hepatic hypovascular nodules that show hyperintensity on T2-weighted images, or that show a higher growth rate should be considered for more frequent follow-up or biopsy.

The aims of our study were to identify patient characteristics and MR imaging findings associated with subsequent hypervascularization in hypovascular nodules that show hypointensity on gadoxetic acid–enhanced hepatobiliary phase MR images in patients with chronic liver diseases.

Materials and Methods

Study Group

Retrospective data collection and analysis were approved by the institutional review board of the two participating hospitals, and the requirement for informed consent was waived. The selection of the subjects is outlined in Figure 1. From February 2008 to October 2010, there were 238 patients who underwent multiple gadoxetic acid–enhanced MR imaging examinations for HCC surveillance. Of these, we excluded patients with *(a)* Child-Pugh class C, owing to insufficient enhancement on gadoxetic acid–enhanced hepatobiliary phase MR images (1), and *(b)* those who had undergone previous systemic chemotherapy or treatment with molecularly targeted agents against malignant tumors. One radiologist (S. Kumano, with 22 years of experience in abdominal imaging) and one gastroenterologist

Published online
10.1148/radiol.12112677 **Content code:** GI

Radiology 2013; 266:480–490

Abbreviations:
CI = confidence interval
HCC = hepatocellular carcinoma
HR = hazard ratio
TVDT = tumor volume doubling time

Author contributions:
Guarantors of integrity of entire study, T.H., T. Murakami; study concepts/study design or data acquisition or data analysis/interpretation, all authors; manuscript drafting or manuscript revision for important intellectual content, all authors; approval of final version of submitted manuscript, all authors; literature research, T.H., Y.I., M.O., Y.K., S. Kumano, M.K., T. Murakami; clinical studies, T.H., Y.I., M.O., Y.K., S. Kogita, M.K.; statistical analysis, T.H., Y.I., M.H.; and manuscript editing, T.H., T. Murakami, Y.I., M.O., M.H., T. Mochizuki.

Conflicts of interest are listed at the end of this article.

Figure 1

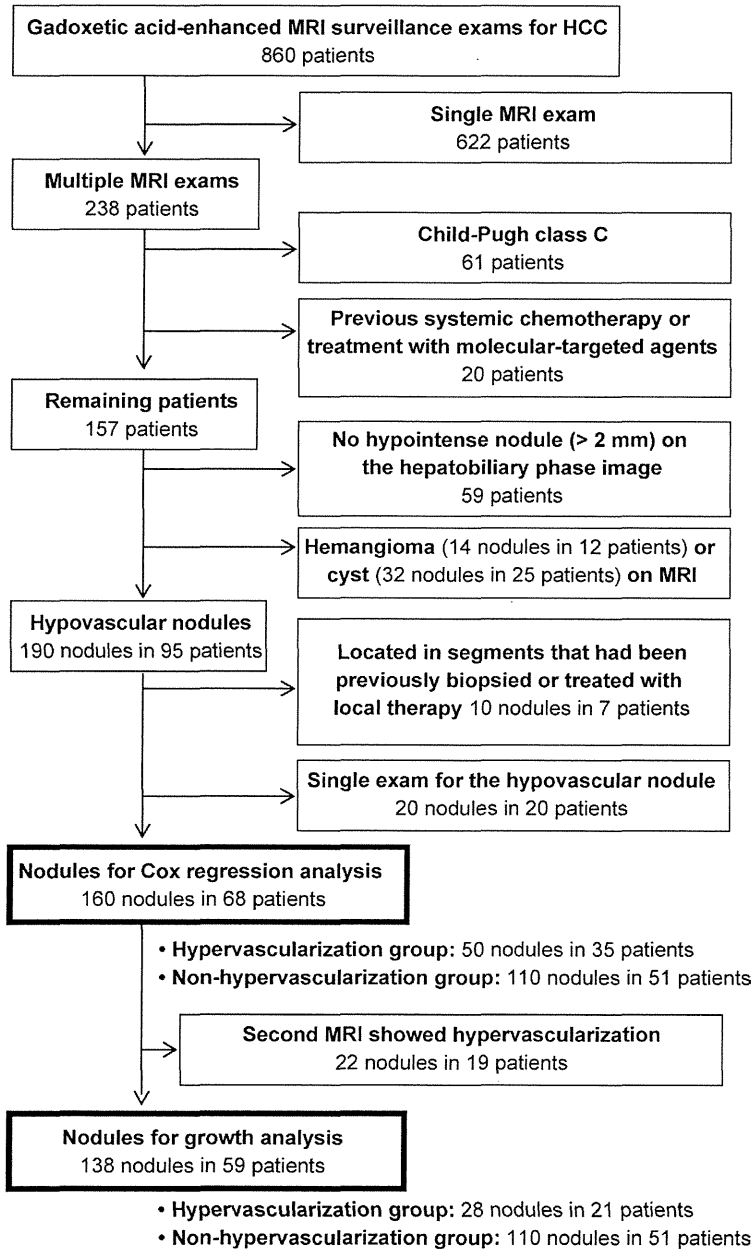

Figure 1: Flowchart of the study population.

specializing in hepatology (Y.I., with 30 years of experience) reviewed images to detect hypovascular nodules and to diagnose subsequent hypervascularization in consensus. A hypovascular nodule was defined as that in which all parts of the nodule showed lower signal intensity than the surrounding liver parenchyma during the arterial phase of dynamic imaging when any of the available modalities were used (intravenous contrast-enhanced CT, CT hepatic arteriography and contrast-enhanced ultrasound) compared with the corresponding site on the unenhanced image. The arterial enhancement was assessed by means of visual inspection. In addition, the subjects were limited to those with round hypointense lesions on gadoxetic acid–enhanced hepatobiliary phase MR images. Procedures involving all modalities were performed within 2 weeks of each other. Nodules were excluded if they were *(a)* less than 2 mm in diameter; *(b)* considered to be suspicious for hemangiomas, cysts or cystic tumors on the basis of other MR imaging sequences or modalities; or *(c)* located in segments that had been previously biopsied or treated with local therapy (including transcatheter arterial chemoembolization).

We identified 160 hypovascular nodules in 68 patients (mean patient age ± standard deviation, 70.0 ± 7.8 years; range, 51–85 years). Among these patients, 48 were men (mean age, 69.9 ± 7.7 years; range, 54–85 years), and 20 were women (mean age, 70.2 ± 8.4 years; range, 51–79 years). The presumed causes of chronic liver disease of the patients were chronic hepatitis C viral infection (n = 46), chronic hepatitis B viral infection (n = 12), alcohol abuse (n = 4), nonalcoholic steatohepatitis (n = 1) and unknown cause (n = 5). Forty (27%) patients had cirrhosis. The number of nodules per patient ranged from one to 10, with a mean value of 2.3. The date of entry into the study was defined as the date of the initial gadoxetic acid–enhanced MR imaging examination. All patients were treated according to the clinical guidelines for the diagnosis and treatment of HCC in Japan (15). During the study period, all patients

received follow-up gadoxetic acid–enhanced MR imaging examinations in combination with US, CT, or angiography at various times according to the degree of liver disease. One radiologist (S. Kumano) and one gastroenterologist who specializes in hepatology (Y.I.) reviewed images in consensus to verify lesion correspondence between the different imaging modalities. Each nodule was followed up until it showed early enhancement when imaged by means of any of the imaging modalities, until the segment containing the nodule was biopsied or treated, or until the final imaging examination of the study period. The number of gadoxetic acid–enhanced MR imaging examinations reviewed per patient was two for 32 patients (43%), three for 16 patients (28%), four for 12 patients (18%), five for three patients (4%), six for three patients (4%), seven for one patient (1%) and eight for one patient (1%). The mean interval between gadoxetic acid–enhanced MR imaging examinations was 186 days ± 110 (range, 57–619 days). Of the 110 nodules that did not develop into hypervascular nodules, 101 were censored at the date of the most recent consultation before November 1, 2010, and nine (in five patients) were censored at the date of the final imaging examination of the study period before therapy (six nodules for transarterial chemoembolization; one each for radiofrequency ablation, intra-arterial reservoir chemotherapy and whole-liver radiation therapy due to coexistent HCC) of the liver segment(s) involved.

We obtained the baseline clinical data by means of review of all available medical records for assessment of the association with the subsequent hypervascularization. The clinical data comprised seven patient characteristics at the time of baseline MR imaging and six initial gadoxetic acid–enhanced MR imaging findings from each nodule (see the Imaging Analysis subsection). Patient characteristics that were used in the study were age, sex, Child-Pugh classification, cause of liver disease, serum α-fetoprotein level, history of local therapy for HCC, and coexistence of hypervascular HCC. For patients with hepatitis B infections, we recorded information regarding the use of oral nucleotide analogs with activity against hepatitis B. The mean interval between the laboratory test and initial MR imaging examination was 9 days (range, 0–24 days).

Nodules were categorized into two groups according to the presence (hypervascularization group) or absence (nonhypervascularization group) of early enhancement at the final imaging examination. Needle biopsy specimens were reviewed by two expert pathologists who made a consensus diagnosis according to the International Working Party criteria (9).

Imaging Techniques

MR imaging studies were performed by using either a 3.0 T (Achieva; Philips Medical Systems, Best, Netherlands) or one of two 1.5 T systems (Signa Excite HDxt; GE Healthcare, Milwaukee, Wis; Gyroscan Intera Nova; Philips Medical Systems) (Table 1). First, a T1-weighted dual-echo sequence was performed. For dynamic imaging, T1-weighted three-dimensional fat-suppressed gradient-echo images were acquired before and after a bolus injection of 0.025 mmol/kg of body weight of gadoxetic acid (EOB-Primovist; Bayer Schering Pharma, Osaka, Japan) at a rate of 2 mL/sec with a saline flush through the antecubital vein. Arterial-phase imaging was performed by using a bolus tracking technique: the center of k-space was acquired 15 seconds after the contrast material appeared in the abdominal aorta (16). Portal venous and hepatobiliary phase images were acquired after an imaging delay of 70 seconds and 20 minutes, respectively. T2-weighted images were acquired with a fat-suppressed fast spin-echo sequence before or within 10 min after contrast-material injection. Although there were missing data from the fat-suppressed T2-weighted fast spin-echo images (not available owing to motion artifacts in two nodules; other T2-weighted sequences were obtained for 32 nodules), we included all subjects in the analysis. Dynamic contrast-enhanced CT, CT hepatic arteriography and contrast-enhanced US were performed as described in the literature (17–19).

Image Analysis

A consensus review of baseline MR images was performed by three radiologists (M.O., T.H., and Y.K., with 18, 11, and 6 years of experience in abdominal imaging, respectively), who were blinded to the outcomes and the biopsy results for each nodule. The fat content of each nodule was determined on the basis of T1-weighted dual-echo images according to apparent signal loss on opposed-phase images relative to in-phase images. On the T2-weighted images, each lesion was evaluated for signal intensity relative to that of the surrounding liver parenchyma and classified as hyperintense, isointense, hypointense or missing. On the T1-weighted three-dimensional fat-suppressed gradient-echo images of without and with contrast enhancement (hepatobiliary phase), signal intensities of the nodule and liver parenchyma were recorded to evaluate nodule-to-liver contrast ratios. For measurement of the nodule, one abdominal radiologist (T.H.) placed the largest possible region of interest but did not include the edges of the nodule to avoid edge artifacts. For the liver parenchyma, two regions of interest that avoided the major hepatic and portal vessels (size range, 200–400 mm^2) were selected, and then the mean value was calculated. The nodule-to-liver contrast ratios were calculated for each unenhanced and hepatobiliary phase image by dividing the signal intensity of the nodule by the signal intensity of the liver parenchyma. The contrast enhancement ratio was then calculated by dividing the contrast ratios of the hepatobiliary phase images by those of the unenhanced images.

One abdominal radiologist (T.H.) measured the maximum nodule diameter on axial gradient-echo T1-weighted gadoxetic acid–enhanced hepatobiliary-phase images of the baseline and the final MR imaging examinations. Only for the purpose of the growth analysis, the final MR imaging examination was defined as the last MR imaging examination before hypervascularization for each nodule. Twenty-two nodules in which the second MR imaging examination showed hypervascularization (19 pairs of examinations; median interval between the two examinations, 210 days;

Table 1

Pulse Sequence Parameters for 1.5-T and 3.0-T Imaging

	T1-weighted Dual-Echo GRE*		Fat-suppressed 3D T1-weighted GRE		Fat-suppressed T2-weighted Fast Spin-Echo	
Parameter	1.5 T 2D†	3.0 T 3D‡	1.5 T†	3.0 T‡	1.5 T†	3.0 T‡
Breathing	Breath hold	Breath hold	Breath hold	Breath hold	Respiratory-triggered technique	Respiratory-triggered technique
Matrix	256 × 256, 320 × 192	192, 176	320 × 512, 320 × 192	320 × 256, 320 × 192	512 × 272, 256 × 224	400, 400
Section thickness (mm)	8, 3.5	7, 7	5, 5	2.5, 3	8, 7	6, 6
Intersection gap (mm)	0.8, 0	0, 0	−2.5, −2.5	−1.25, −1.5	0.8, 1.4	1, 1
Repetition time (msec)	200, 200	3.9, 3.8	4.4, 4.3	3.5, 3.5	>2000, >2000	>3000, >3000
Echo time (msec) in/opposed	4.6/2.3, 4.3/2.1	1.17/2.5, 1.17/2.5	2.2, 2.1	1.7, 1.7	80, 105	80, 80
Flip angle/refocusing angle (degrees)	70, 70	10, 10	10, 12	10, 10	180, 180	160, 160
Reduction factor	1.8, 2	2, 2	1.8, 2	2, 1.9	0, 2	1.6, 2

Note.—Field of view was 250–270 mm × 350–380 mm (adjusted for each patient). 2D = two dimensional, 3D = three dimensional, GRE = gradient-recalled echo.

* Indicates in- and opposed-phase imaging.

† For the 1.5-T system, a 16-channel and an 8-channel phased-array body coil were used. Data are presented as 16 channel/8 channel.

‡ For the 3-T system, a 6-channel body coil and 32-channel cardiac coil were used and adjusted to the patient's physique. Data are presented as 6 channel/32 channel.

range, 91–410 days) were excluded from the growth analysis, because the growth rate before hypervascularization could not be calculated. Thus, 138 nodules from 59 patients were included in the growth analysis. First, the tumor volume doubling time (TVDT) was calculated as follows (20,21): TVDT = $T \times \log 2/[3 \times \log(D_2/D_1)]$, where T is the time interval between two measurements and D_1 and D_2 denote the maximum diameter of the nodule at the initial and last MR imaging examinations, respectively. Then, the growth rate of the nodules was calculated as the inverse of the TVDT.

Statistical Analysis

All analyses were conducted at the nodule level. R software (Version 2.12.0; R Foundation for Statistical Computing, Vienna, Austria) was used for statistical analysis (22). To evaluate the independent prognostic significance of baseline covariates for subsequent hypervascularization, a multivariate Cox proportional hazard model was used. Because 32 patients had multiple nodules detected at two or more follow-up examinations, we used the coxph function from the survival package in the R software, with the cluster option. This method allows accounting for correlation induced by having multiple nodules per patient and uses robust variance estimates (23). Before model selection, bivariate analysis was performed by using Spearman rank correlations to test for collinearity among independent variables. As a result, Spearman correlation coefficients for variables were generally below 0.5, which suggests that multicollinearity was not of concern. Hazard ratios (HRs) and 95% confidence intervals (CIs) were calculated. Because no factor (except intensity on T2-weighted images) was found to show a significant difference when univariate analysis was performed, preliminary multivariate Cox proportional hazards models were constructed by using all 13 variables. Candidate variables were then allowed to enter the final model (entry criterion, $P < .05$). Fat content and initial diameter were forced into the final model because they were considered important predictors (12). The Wald test was performed to determine an overall P value for each variable, and a robust score test was used to assess the significance of the final model as a whole. The model that was fitted by using missing data was not appreciably different from that with the missing data excluded.

The median time interval between the initial and final MR imaging examination was compared for the two groups by using the Mann-Whitney U test. For evaluation of initial diameter and growth rate of the nodules, continuous data differences between the two groups were tested with the Mann-Whitney U test, and categorical data were assessed by using the χ^2 test. Correlation between the initial diameter and the growth rate of the nodules was examined by using the Kendall tau rank test. The prognostic value of the growth rate was evaluated by means of the area under the receiver operating characteristic curve. By using the ROCR package in the R software, the cutoff value for the growth rate was determined at the optimal operating point, with the highest sensitivity and specificity combined (24). Cumulative event rates were estimated by using the Kaplan-Meier method and compared by using the log rank statistic. A P value of less than .05 was considered to indicate a statistically significant difference. All P values were two-sided.

Results

Study Population and Events

During the median follow-up time of 342 days (range, 64–948 days), arterial hypervascularization was observed in 31% (50 of 160) of the nodules in 52% (35 of 68) of the patients. The cumulative percentages of nodules that showed

Table 2

Baseline Patient Characteristics and MR Imaging Findings of 160 Nodules

Parameter	No. of Nodules	Hypervascularization at Follow-up		Preliminary Multivariate Cox Model	
		Yes (n = 50)	No (n = 110)	HR (95% CI)	P Value
Patient characteristic					
Age (y)	...	70.5 ± 7.6 (58–85)*	70.4 ± 8.3 (51–84)*	1.0 (0.9, 1.1)	.852
Sex	...				.326
Men	106	32 (30)	74 (70)	1.0	
Women	54	18 (33)	36 (67)	1.4 (0.7, 3.1)	
Child-Pugh class					.005
A or chronic hepatitis	146	44 (30)	102 (70)	1.0	
B	14	6 (43)	8 (57)	3.8 (1.5, 9.0)	
Etiology of liver disease					.019
Hepatitis C virus	107	35 (33)	72 (67)	1.0 (0.3, 3.1)	
Hepatitis B virus	26	6 (23)	20 (77)	0.2 (0.03, 0.8)	
Non-B, non-C (ref)	27	9 (33)	18 (67)	1.0	
Serum α-fetoprotein level > 20 ng/mL	66	24 (36)	42 (64)	0.9 (0.5, 2.0)	.948
History of local therapy for HCC	129	46 (36)	83 (64)	5.5 (2.1, 14.7)	<.001
Coexistence of hypervascular HCC	67	29 (43)	38 (57)	2.0 (1.1, 3.7)	.022
MR Imaging Finding					
Fat-suppressed T2-weighted fast spin echo†					<.001
Hyperintensity	18	10 (56)	8 (44)	9.4 (3.6, 24.5)	
Iso- or hypointensity (ref)	108	25 (23)	83 (77)	1.0	
Missing data	34	15 (34)	19 (56)	3.7 (1.7, 8.0)	
Fat containing on in- and opposed-phase images†	24	10 (42)	14 (58)	1.4 (0.6, 3.4)	.491
Noise-to-liver contrast on unenhanced fat-suppressed T1-weighted GRE images	...	0.95 ± 0.14 (0.66–1.3)*	0.97 ± 0.17 (0.49–1.9)*	0.05 (0.1×10^{-4}, 1.7×10^{2})	.464
Noise-to-liver contrast on hepatobiliary phase fat-suppressed T1-weighted GRE images	...	0.69 ± 0.13 (0.31–0.99)*	0.71 ± 0.11 (0.46–0.95)*	47.5 (6.8×10^{-4}, 3.3×10^{6})	.489
Gadoxetic acid contrast-enhancement ratio	...	0.74 ± 0.14 (0.40–0.98)*	0.75 ± 0.14 (0.42–1.5)*	0.07 (0.1×10^{-5}, 3.8×10^{3})	.629
Diameter (mm)	...	9.5 ± 5.1 (2–34)*	9.8 ± 3.7 (4–21)*	1.0 (0.9, 1.1)	.998

Note.—Unless otherwise indicated, data are numbers of patients, with percentages in parentheses. GRE = gradient-recalled echo, ref = referent category.

* Data are mean ± standard deviation, with range in parentheses.

† Qualitative assessment.

hypervascularization at 6, 12, 18, and 24 months were 10%, 25%, 36%, and 46%, respectively. Hypervascularization was diagnosed in 39 nodules on the basis of arterial-phase gadoxetic acid–enhanced MR images, eight nodules on the basis of dynamic CT images, two nodules on the basis of CT hepatic arteriographic images, and one nodule on the basis of contrast-enhanced US. In the hypervascularization group, the mean number of hypervascularized nodules was 1.5 (range, 1–7) per patient during the study period.

Histologic results from core needle biopsy were obtained for 13 nodules. Of these, nine nodules were in the hypervascularization group (eight well-differentiated HCCs and one moderately differentiated HCC). Three nodules in the nonhypervascularization group were diagnosed as dysplastic nodules and one as well-differentiated HCC.

Baseline Findings

Table 2 shows the baseline characteristics of the 160 nodules and results of the preliminary multivariate Cox regression. In the final model, five of the variables showed a statistically significant difference (robust score test, P = .023; Table 3). The factors associated with an increased risk of hypervascularization were hyperintensity on T2-weighted images (HR = 8.7; 95% CI: 3.6, 20.8), previous local therapy for HCC (HR = 5.0; 95% CI: 1.8, 13.6), Child-Pugh class B cirrhosis (HR = 3.6; 95% CI: 1.4, 9.5), and coexistence of hypervascular HCC (HR = 2.0; 95% CI: 1.0, 3.8). Hepatitis B infection was independently associated with a decreased risk (HR = 0.2; 95% CI: 0.04, 0.8). Of 26 nodules in 13 patients with chronic hepatitis B infections, 23 nodules in 11 patients were treated with oral nucleotide analogs with activity against hepatitis B at the point of entry (five of six nodules in the hypervascularization group and 18 of 20 nodules in the nonhypervascularization group). Fat content and the initial diameter of the nodule were not substantially different in the final model. Of 14 fat-containing nodules in the nonhypervascularization

group, four nodules in one patient were censored because the patient underwent transcatheter arterial chemoembolization for HCC in a different liver segment. Two nodules were censored because of biopsy; one was diagnosed as moderately differentiated HCC, and the other was a dysplastic nodule. The mean initial nodule diameter was not significantly different between the hypervascularization (9.5 mm ± 5.1 [range, 2–34 mm]) and the nonhypervascularization groups (9.8 mm ± 3.7 [range, 4–21 mm]) (P = .282). The numbers of nodules that were smaller than 5 mm, 5–10 mm, 10–15 mm, and greater than 15 mm in initial size were four, 28, 11, and seven in the hypervascularization group, and three, 60, 33, and 14 in the nonhypervascularization group, respectively. In addition, there was no difference in the percentage of nodules greater than or equal to 15 mm in size between the two groups (14% [seven of 50] vs 13% [14 of 110], respectively; P = .825).

Table 3

Multivariate Predictors of Subsequent Hypervascularization

Variable	HR (95% CI)	*P* Value
Significant independent predictors		
Child-Pugh classification		.008
A or chronic hepatitis	1.0	
B	3.6 (1.4, 9.5)	
Cause of liver disease		.017
Hepatitis C virus	1.1 (0.4, 3.1)	
Hepatitis B virus	0.2 (0.04, 0.8)	
Non-B and non-C liver disease (Ref)	1.0	
History of local therapy for HCC	5.0 (1.8, 13.6)	.002
Coexistence of hypervascular HCC	2.0 (1.0, 3.8)	.038
Fat-suppressed T2-weighted fast spin echo		<.001
Hyperintensity	8.7 (3.6, 20.8)	
Hypo- or isointensity (Ref)	1.0	
Missing data	3.4 (1.4, 7.9)	
Additional variables included in the model		
Fat containing on in- and opposed-phase images	1.3 (0.5, 3.7)	.567
Diameter (mm)	1.0 (0.9, 1.1)	.692

Growth Analysis

Twenty-eight lesions in the hypervascularization group (initial diameter, 9.7 mm ± 5.9 [range, 2–34 mm]) and 110 nodules (9.8 mm ± 3.7 [range, 4–21 mm]) in the nonhypervascularization group were evaluated. The median time between the initial and last MR imaging examination was not significantly different (P = .075) between the two groups (235 and 293 days, respectively). In the hypervascularization group, 27 nodules increased in diameter during follow-up (Fig 2) and one remained stable. The mean growth rate in the hypervascularization group (6.5×10^{-3}/day [TVDT, 154 days]) was significantly higher ($P = 1.8 \times 10^{-6}$) than that in the nonhypervascularization group (1.1×10^{-3}/day [TVDT, 946 days]) (Fig 3). There was no correlation between initial diameter and growth rate (Kendall tau = −0.066; P = .266) (Fig 4). Receiver operating characteristic analysis (area under the curve, 0.79) identified a growth rate cutoff value of 1.8×10^{-3} per day (TVDT, 542 days) with a positive predictive value of 89% (25 of 28 nodules) and a negative predictive value of 63% (70 of 110 nodules) for hypervascularization (Fig 5, *A*). The 1-year cumulative proportion of nodules showing hypervascularization was 0% for those with a growth rate of less than 1.8×10^{-3}/day and 53% for those with a growth rate greater than or equal to 1.8×10^{-3}/day (log-rank test, $P = 5.2 \times 10^{-8}$; Fig 5, *B*).

Discussion

We set out to determine risk factors associated with hypervascularization in hypovascular nodules in patients with chronic liver diseases by using time-to-event analysis. Among the baseline patient characteristics and MR imaging findings, the most important variable associated with an increased risk of hypervascularization was hyperintensity on T2-weighted images. In the hypervascularization group, higher signal intensity on T2-weighted images might reflect peliotic changes in the intratumoral sinusoids of HCC (25). Meanwhile, nodular regeneration, fibrosis, and scarring that occur in the course of cirrhosis occasionally appear as hyperintense round lesions on T2-weighted images. Dysplastic nodules can be hyperintense on T2-weighted images; the causes are considered to be varying degrees of fibrosis, or infarction (26,27). It has been reported that T2-weighted imaging does not provide added diagnostic value to gadoxetic acid–enhanced images for the detection and characterization of focal lesions in cirrhotic livers (28). Findings from our study suggest that the combination of T2-weighted images and gadoxetic acid–enhanced MR images could be useful in the prediction of hypervascularization of previously hypovascular nodules.

Child-Pugh class B cirrhosis increased the risk of hypervascularization compared with Child-Pugh class A or chronic hepatitis, and hepatitis B infection decreased the risk compared with hepatitis C infection. These results might reflect the epidemiologic features of HCC (29,30); Child-Pugh class B and C are associated with a three-fold increase in the risk of HCC. The annual incidence of HCC in patients with cirrhosis due to hepatitis B infection exceeds 2%, which is lower than that due to hepatitis C infection (3%–8%). In addition, there may be morphologic and histologic differences between hypovascular nodules associated with hepatitis B and those associated with hepatitis C infection.